Progress In Electromagnetics Research, PIER 96, 329–346, 2009

NARROWBAND FILTER IN A HETEROSTRUCTURED MULTILAYER CONTAINING ULTRATHIN METALLIC FILMS

C.-C. Liu

Graduate School of Engineering Science and Technology
National Yunlin University of Science and Technology
Douliou, Yunlin 640, Taiwan

Y.-H. Chang

Department and Graduate School of Electronic Engineering
National Yunlin University of Science and Technology
Douliou, Yunlin 640, Taiwan

T.-J. Yang

Department of Electrical Engineering
Chunghua University
Hsinchu 300, Taiwan

C.-J. Wu

Institute of Electro-Optical Science and Technology
National Taiwan Normal University
Taipei 116, Taiwan

Abstract—A narrowband reflection and/or transmission filter made of heterostructured multilayer with two different ultrathin metallic films is proposed. The multilayer structure is a cascaded system that is formed by using two narrowband reflection-and-transmission filters. Each individual filter is made of an ultrathin metal film in front of a planar Fabry-Perot resonator. Using the transfer matrix method in a stratified system, the optical filtering properties are theoretically investigated and analyzed. It is found that the reflection peak at the design wavelength in the original individual filter becomes a dip in the heterostructured filter. The role played by the stack number of Bragg reflector in the design of narrowband filter is also clearly elucidated.

Corresponding author: C.-J. Wu (jasperwu@ntnu.edu.tw).

1. INTRODUCTION

It is known that a common dielectric multilayer narrowband transmission filter or Fabry-Perot filter (FPF) can be designed and achieved by inserting a defect layer in a Bragg reflector (BR). The structure of this FPF with a central defect L is denoted as $\mathrm{Air}/(HL)^N L(HL)^N/\mathrm{Air}$, in which the number of periods is N, and H and L are respectively the high- and low-index (n_H and n_L) of dielectric layers with optical thickness being equal to the quarter-wavelength, i.e., $n_H d_H = n_L d_L = \lambda_0/4$, where λ_0 is the design wavelength, and d_H, d_L are the physical thickness of H and L, respectively. The location of the transmission narrowband is usually designed to be in the vicinity of center of the high-reflectance band. A narrowband FPF can be used as a frequency-selective filter which is an important device in signal processing. It can also work as a demultiplexer for the wavelength division multiplexing (WDM) systems. The related optical properties for such a multilayer FPF are well described in an excellent book of electromagnetic waves [1].

The above-mentioned typical FPF is all-dielectric, i.e., all the constituent layers are dielectrics. In addition, the total number of layers in the whole system is generally very large because the number of periods in the BR should be sufficiently large for the purpose of producing the so-called high-reflection band, or the photonic bandgap (PBG). The BR with large number of periods is, in effect, also referred to as a one-dimensional photonic crystal (PC). Thus, with a large total number of layers in a typical FPF, it is difficult to monitor the multilayer coating experimentally. In order to reduce the number of periods in the constituent BRs, a new design of multilayer narrowband filter with a small number of periods and an ultrathin metallic film is proposed and now is feasible [2–8]. For instance, a filter structure like $\mathrm{Air}/\mathrm{Cr}(LH)^{m_1}\,2L\,(HL)^{m_2}\,H/\mathrm{Sub}$, that is made of an ultrathin metallic film, Cr, in front of an FPF, i.e., is depicted in Fig. 1 [6–8], where the numbers of periods of the BRs are m_1 and m_2. In addition, H and L are again the quarter-wavelength layers of the high- and low-index materials, and Sub is the substrate. This structure is a narrowband filter that can be in both reflection and transmission because it exhibits simultaneous peaks in both the wavelength-dependent reflectance and transmittance at the design wavelength. To attain the peaks in the reflectance and transmission, three specified conditions should be satisfied. First, the thickness of Cr must be ultrathin and much less than the design wavelength, i.e., $d \ll \lambda_0$. Second, the complex-valued refractive index of Cr, $n_{\mathrm{Cr}} = n_R - jn_I$, must have the comparable real and imaginary parts,

i.e., $n_R \approx n_I$. Third, the numbers of periods of two BRs will be limited to $m_1 \leq m_2$. Although, due to the substantial absorption in the metal film, neither the reflectance can reach so high as that of in a PC nor the transmittance is equal to one as in a usual FPF; such a kind of filter possesses a unique feature of the simultaneous peaks in the reflectance and the transmittance as well. A filter with such a property is promising for the optical applications. For example, in the optical signal processing one can use one channel as a reference signal and the other as a probing signal. It can also be used as a color decoration device because the colors in the reflected and transmitted light are similar.

On the other hand, in order to get a wider photonic bandgap in a one-dimensional photonic crystal, the heterostructured photonic crystals have been proposed and investigated recently [9–13]. The heterostructure formed by cascading two PCs is proven to be able to enlarge the PBG. With the idea of photonic heterostructure, in this paper, we try to investigate the filtering properties for a heterostructured narrowband filter formed by cascading two structures in Fig. 1 with different metal films such as Cr and Fe. The optical reflectance, transmittance, and absorptance will be calculated by making use of the transfer matrix method (TMM) [14]. Discussion on the filtering properties for such a heterostructured narrowband filter will be given.

2. BASIC EQUATIONS

The heterostructured narrowband filter to be considered in this paper is Air/Cr$(LH)^{m_1}2L(HL)^{m_2}H$ Fe$(LH)^{m_1}2L(HL)^{m_2}H$/Sub, which can be viewed as a system cascaded by two subsystems shown in Fig. 1. According to TMM, the transmittance and reflectance can

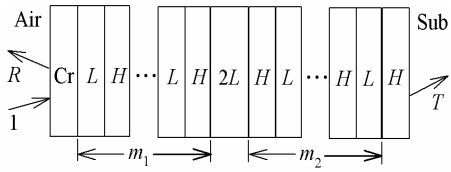

Figure 1. A structural diagram for the narrowband reflection and transmission filter, in which an ultra thin metallic film, Cr, is deposited on an FPF which is made of a low-index layer, $2L$, sandwiched by two Bragg reflectors with numbers of periods denoted by m_1 and m_2, respectively. Here R and T are the optical reflectance and transmittance, respectively.

be determined by the matrix of the entire system given by

$$\begin{aligned} M &= \begin{pmatrix} M_{11} & M_{12} \\ M_{21} & M_{22} \end{pmatrix} \\ &= D_0^{-1} M_{\mathrm{Cr}} \left(M_L M_H\right)^{m_1} M_{2L} \left(M_H M_L\right)^{m_2} M_H M_{\mathrm{Fe}} \left(M_L M_H\right)^{m_1} \\ &\quad M_{2L} \left(M_H M_L\right)^{m_2} M_H D_{\mathrm{Sub}}, \end{aligned} \tag{1}$$

where the layer matrix in each layer is given by

$$M_\ell = D_\ell P_\ell D_\ell^{-1}, \tag{2}$$

with $\ell = \mathrm{Cr}$, L, H, $2L$, and Fe. Then the reflectance R and transmittance T are determined by two matrix elements M_{11} and M_{21} and are expressed as

$$R = \left|\frac{M_{21}}{M_{11}}\right|^2, \tag{3}$$

$$T = \frac{n_{\mathrm{sub}} \cos\theta_{\mathrm{sub}}}{n_{\mathrm{air}} \cos\theta_{\mathrm{air}}} \left|\frac{1}{M_{11}}\right|^2. \tag{4}$$

The absorptance A, which is defined as the fraction of energy dissipated in the metallic films, is then given by

$$A = 1 - R - T. \tag{5}$$

If the temporal part, $\exp(j\omega t)$, is taken for all fields, then the translational matrix in Eq. (2) for each layer is expressible as

$$P_\ell = \begin{pmatrix} e^{i\phi_\ell} & 0 \\ 0 & e^{-i\phi_\ell} \end{pmatrix}, \tag{6}$$

where the phase parameter is

$$\phi_\ell = k_{\ell x} d_\ell = \frac{2\pi d_\ell}{\lambda} n_\ell \cos\theta_\ell, \tag{7}$$

where the x-direction is the normal direction of the system. In addition, the dynamical matrix in each layer is defined by

$$D_\ell = \begin{pmatrix} 1 & 1 \\ n_\ell \cos\theta_\ell & -n_\ell \cos\theta_\ell \end{pmatrix}, \tag{8}$$

for TE wave, and

$$D_\ell = \begin{pmatrix} \cos\theta_\ell & \cos\theta_\ell \\ n_\ell & -n_\ell \end{pmatrix}, \tag{9}$$

for TM wave, respectively. The incident angle is θ_{air}, while the ray angle in each layer can be determined by the Snell's law of refraction.

Before we present the numerical results, let us mention TMM in dealing with the optical reflection and transmission in a one-dimensional stratified medium. Eqs. (1)–(9) derived by Yeh [14] have been widely employed not only for the usual material but also for recent metamaterials [15]. In fact, there is another elegant version of TMM called Abeles theory [16, 17], which is also familiar in the community.

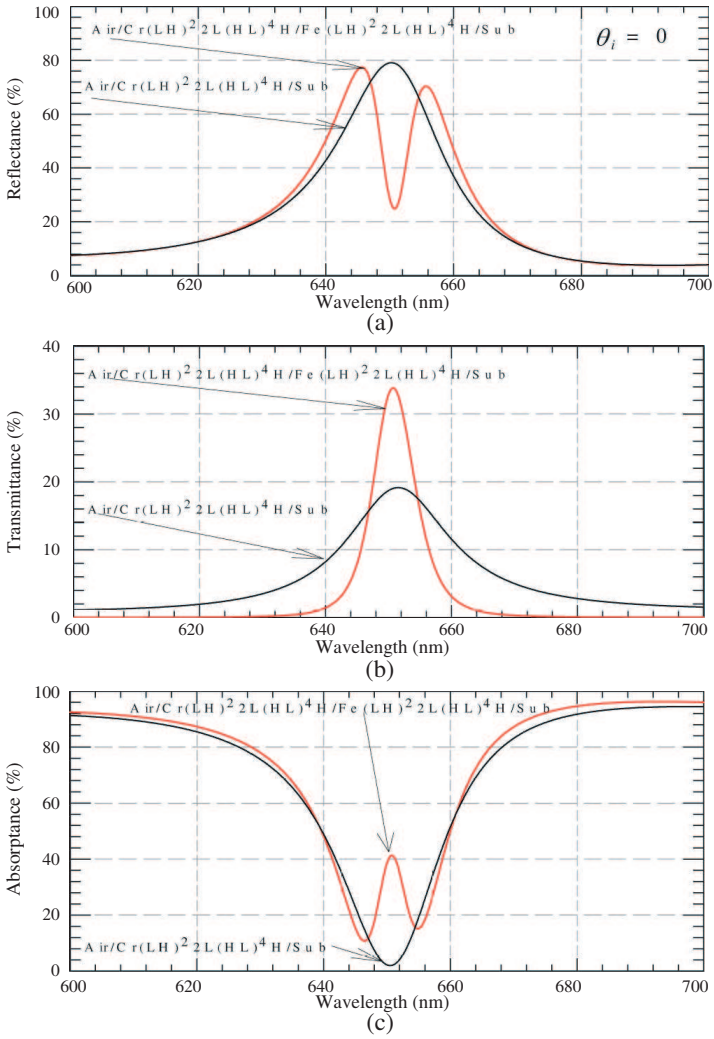

Figure 2. The wavelength-dependent reflectance (a), transmittance (b), and absorptance (c) in the normal incidence. The black curve is for Filter-I, while the red is for Filter-II (red).

Both methods, in fact, yield exactly the same results in the reflection and the transmission as well. Using Abeles theory, the formulation for the current heterostructured filter is also given in the appendix.

3. NUMERICAL RESULTS AND DISCUSSION

In what follows we shall present the numerical results for the heterostructured filter, Air/Cr$(LH)^{m_1}2L(HL)^{m_2}H$ Fe$(LH)^{m_1}2L(HL)^{m_2}H$/Sub. For the convenience of comparison, the filter in Fig. 1 is referred to as Filter-I, while the heterostructured filter is Filter-II. In this study, the design resonant wavelength is taken to be $\lambda_0 = 650\,\text{nm}$. For the metallic layer Cr, a thickness of $d = 5\,\text{nm}$ and an index of refraction $n_{\text{Cr}} = 3.67 - j4.365$ near λ_0 are taken. For Fe, we use $d = 5\,\text{nm}$ and $n_{\text{Fe}} = 2.88 - j3.37$ near λ_0. It should be noted that although the metallic refractive index is wavelength-dependent, it will be a slowly varying function of the wavelength in the current range of interest [7, 8]. The index of refraction of a metal has a severe variation only near the plasma frequency (in the ultraviolet region) according to the Drude model [17]. In the current visible region, the frequency is much less than plasma frequency. Thus, it is reasonable to assume that the refractive indices of Cr and Fe are constant. Additionally, the indices of refraction for quarter-wavelength layers L and H are $n_L = 1.45$ (SiO_2) and $n_H = 2.17$ (TiO_2), respectively. The substrate's refractive index is of the value of glass, i.e., $n_{\text{sub}} = 1.52$.

In Fig. 2, we plot, under the normal incidence, (a) the calculated reflectance, (b) transmittance, and (c) absorptance for the Filter-I (black) and Filter-II (red). Here we have used $m_1 = 2$ and $m_2 = 4$. The effects coming from the heterostructure are seen. The reflectance peak in Filter-I now becomes a dip for Filter-II at the design wavelength λ_0, while the transmittance remains a peak with an enhanced magnitude. The appearance of dip in R causes to generate double resonant peaks in the vicinity of the λ_0. The behavior in R is reflected in the variation of A, in which it becomes a peak at the design wavelength. Thus, the additional metallic film of Fe in Filter-II has strongly influenced the behavior of the reflection, changing from a narrowband reflection filter to a narrowband reflection band-rejected filter. In addition, the double peaks in R could be used as reflective wavelength multiplexer. As for the transmission, the heterostructure has an effect of amplification in T, leading to a larger transmittance. This would be beneficial to the extraction of the designed component of the signal.

The angular dependence of (a) R, (b) T, and (c) A for the heterostructured Filter-II in the TE-wave are plotted in Fig. 3. It can be seen that the increase in the incident angle will cause the

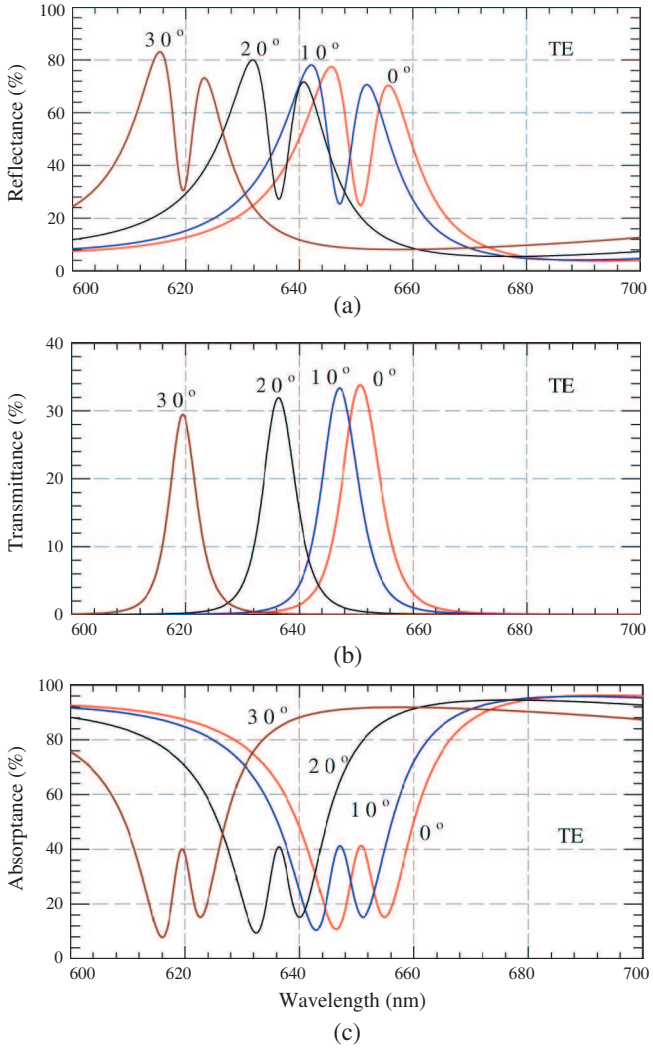

Figure 3. The calculated TE-wave wavelength-dependent reflectance (a), transmittance (b), and absorptance (c) for Filter-II at four different incident angles.

wavelength spectrum to move to the shorter wavelength. That is, the design resonant wavelength can be tuned by changing the incident angle. The angle-dependent R, T, and A in Filter-II are similar to those in Filter-I [8]. In addition to the shifting property, the peak heights for the double peaks in R are slightly enhanced due to the

increase in the angle. Conversely, the peak height in T is decreased with increasing angle. The corresponding results for the TM-wave are plotted in Fig. 4. Similar shifting behaviors can be seen for the TM-wave, which are consistent with those in [8].

The recent report on Filter-I has pointed out that the stack

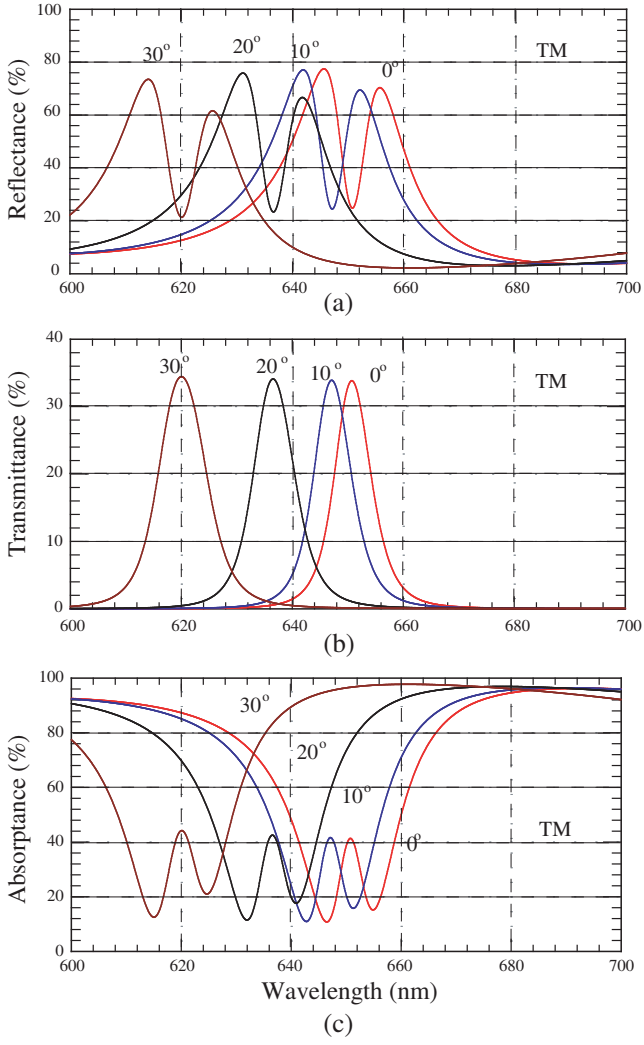

Figure 4. The calculated TM-wave wavelength-dependent reflectance (a), transmittance (b), and absorptance (c) for Filter-II at four different incident angles.

numbers m_1 and m_2 in two BRs have strong influence in the peak height of both R and T [7]. It is our next step to investigate the effects of the stack numbers m_1 and m_2 on R, T and A for the heterostructured Filter-II. First, taking $m_1 = m_2 = 4$, the calculated R, T, and A for the TE-wave are respectively plotted in Fig. 5. Comparing with Fig. 2(a) for 0° we see that the double peaks are more asymmetric about $\lambda_0 = 650\,\text{nm}$. Moreover, the peak height is significantly lowered

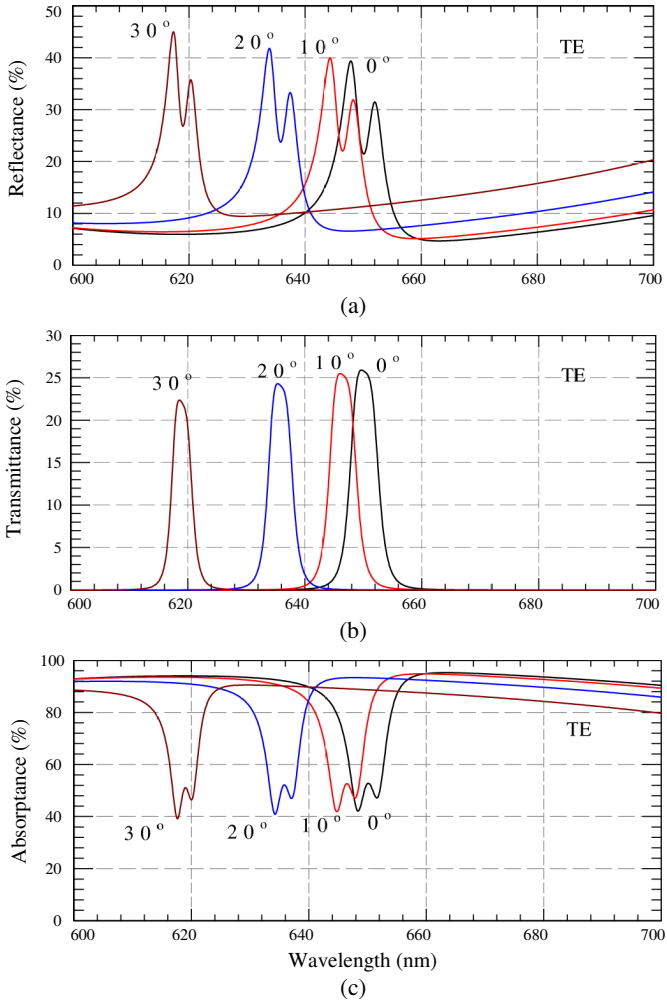

Figure 5. The calculated TE-wave wavelength-dependent reflectance (a), transmittance (b), and absorptance (c) for Filter-II at $m_1 = m_2 = 4$ at four different incident angles.

down, such as from ∼80% to ∼40% for the left peak. The decrease in R will cause T to be increased, as illustrated in Fig. 5(b). The corresponding results for the TM are plotted in Fig. 6, in which the shifting features in R, T, and A are seen again.

If we now take $m_1 = 4$ and $m_2 = 2$, the results are shown in Fig. 7. It is seen that the double-peak shape in R no longer exists. There is only one broad peak with position being shifted to

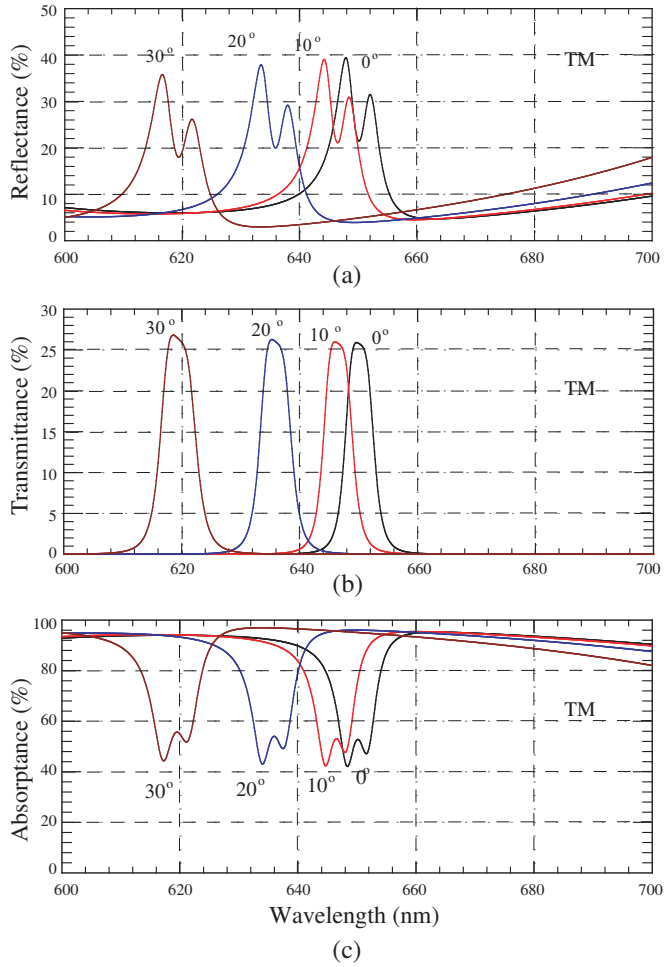

Figure 6. The calculated TM-wave wavelength-dependent reflectance (a), transmittance (b), and absorptance (c) for Filter-II at $m_1 = m_2 = 4$ at four different incident angles.

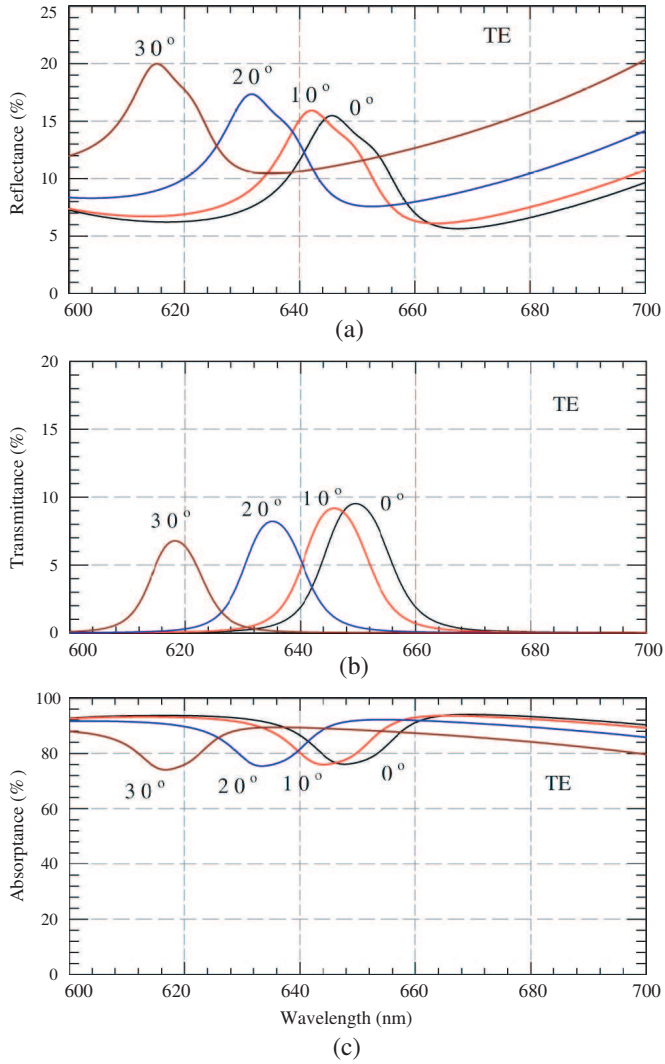

Figure 7. The calculated TE-wave wavelength-dependent reflectance (a), transmittance (b), and absorptance (c) for Filter-II at $m_1 = 4$ and $m_2 = 2$ at four different incident angles.

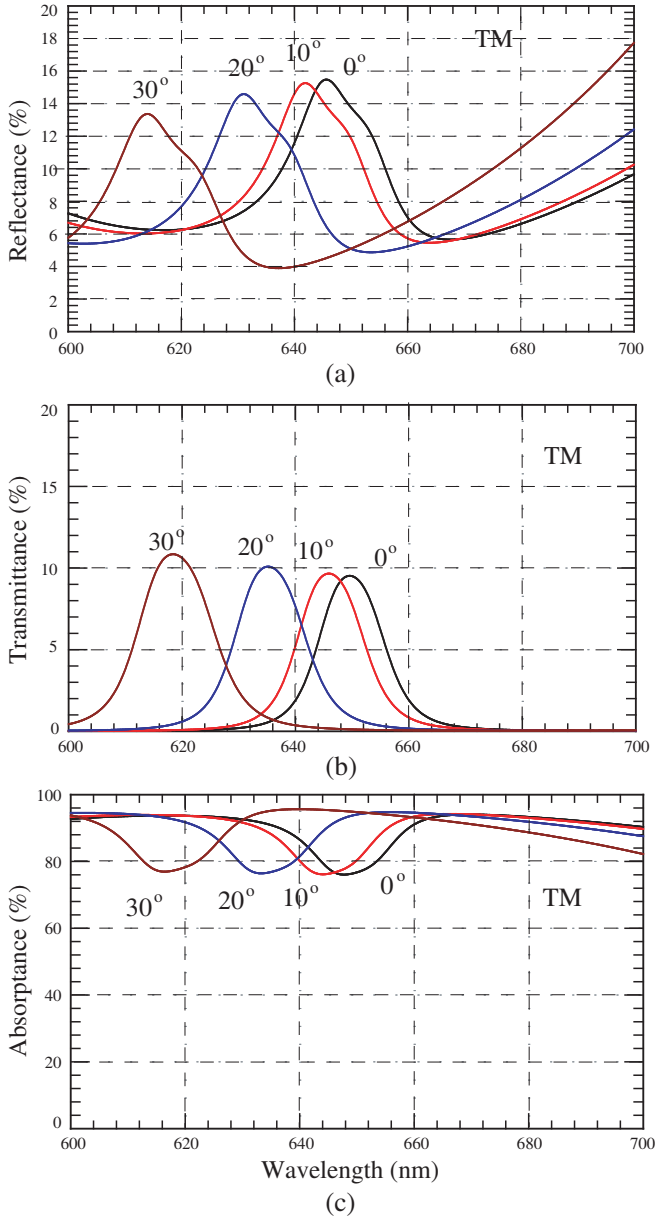

Figure 8. The calculated TE-wave wavelength-dependent reflectance (a), transmittance (b), and absorptance (c) for Filter-II at $m_1 = 4$ and $m_2 = 2$ at four different incident angles.

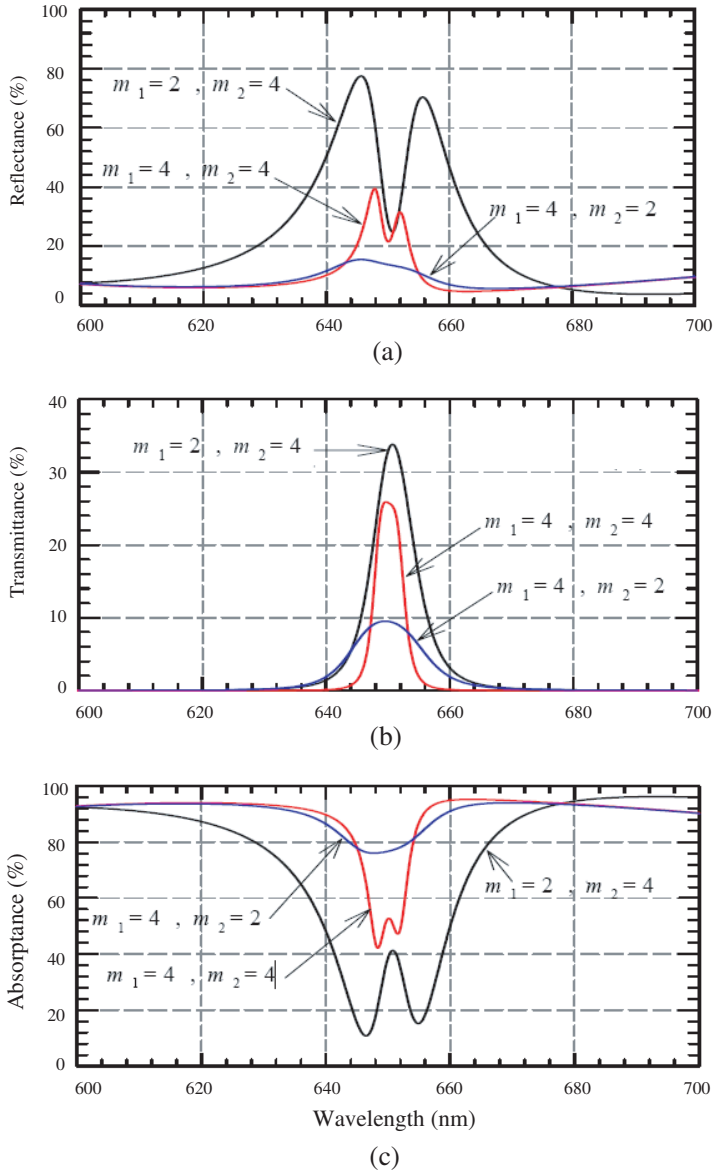

Figure 9. The calculated normal-incidence wavelength-dependent reflectance (a), transmittance (b), and absorptance (c) for Filter-II at three different values in m_1 and m_2.

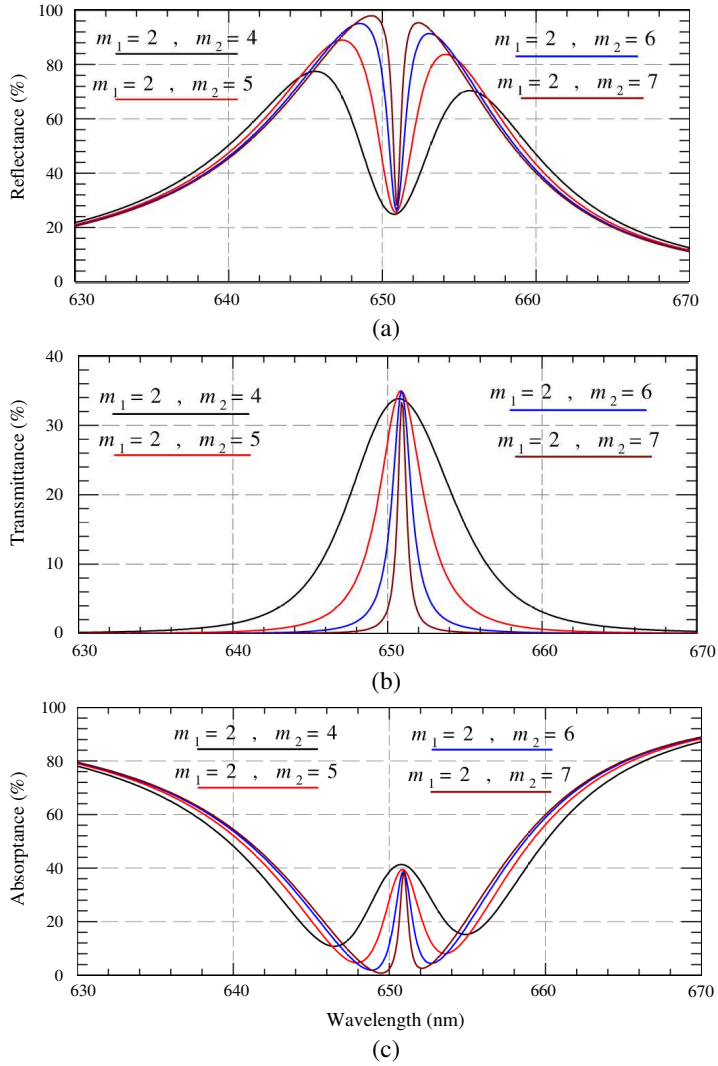

Figure 10. The calculated normal-incidence wavelength-dependent reflectance (a), transmittance (b), and absorptance (c) for Filter-II at four different values in m_1 and m_2 with $m_1 < m_2$.

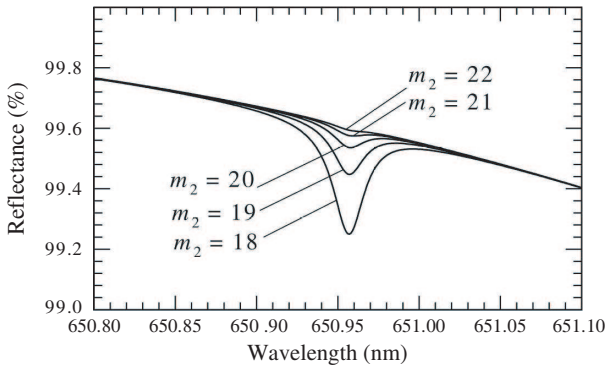

Figure 11. The calculated normal-incidence wavelength-dependent reflectance for Filter-II at five different values in m_2 with $m_1 = 2$. It is seen the dip in R disappears and the double peaks are merged.

the wavelength smaller than the design wavelength. The peak height is also strongly lowered down to ∼16%. The transmittance peak position, however, is not changed in this case, and only the peak height is also significantly decreased. The decrease in both R and T is due to the strong absorptance, as seen in Fig. 7(c), where A is enhanced above 70%, especially in the region near λ_0. The results suggest that the condition of $m_1 \leq m_2$ must also be fulfilled in order to achieve the narrowband filter for the heterostructured one. In addition, the corresponding results of TM-wave are given in Fig. 8. The conclusive results at 0° for three different values of m_1 and m_2 are illustrated in Fig. 9.

The condition of $m_1 \leq m_2$ is further examined as follows. Taking a fixed value of $m_1 = 2$ and changing m_2 as 4, 5, 6, and 7, the calculated R, T, and A are now plotted in Fig. 10. It can be seen that the dip in R and peak in T are significantly narrowed down when the difference, $m_2 - m_1$, is increased. That is, the double peaks in R are even closer to each other. Thus, an ultra narrowband filter can be expected as m_2 increases. There will be the next question coming from the narrowing effect. Is it possible that the double peaks merge together as a single peak when we continue to increase the number of m_2. The answer is clearly replied in Fig. 11, in which the dip disappears, and the double peaks are merged as a peak when $m_2 = 22$. In this case, a reflection and transmission filter as in Fig. 1 is recovered again.

4. CONCLUSION

The optical properties for a heterostructured filter with two metallic films, Air/Cr$(LH)^{m_1}2L(HL)^{m_2}H$ Fe$(LH)^{m_1}2L(HL)^{m_2}H$/Sub, have been investigated. Comparing with the single stage Filter-I, the heterostructure Filter-II has a salient influence in the reflectance, leading to double peaks and a narrow band-reject filter in the reflection. The peak height in the transmittance is also enhanced due to the heterostructure. The effects of the stack numbers m_1 and m_2 are also illustrated numerically. The roles played by these two numbers are elucidated for such a narrowband filter.

In this study, we have investigated the filtering properties operated in the visible region. It is easy to design this kind of filter to be operated in the infrared region by selecting the metallic refractive index or by changing metallic film to other possible materials. This together with the presence of double peaks in the reflectance in the heterostructured filter could serves as a useful wavelength multiplexer in the optical communication. We are going to explore this issue.

APPENDIX A.

According to Abeles theory, the characteristic matrix of the heterostructured Filter-II is the resultant of the product of the individual 2×2 matrices, that is,

$$M = \begin{pmatrix} m_{11} & m_{12} \\ m_{21} & m_{22} \end{pmatrix} = M_{\mathrm{Cr}} \left(M_L M_H\right)^{m_1} M_{2L} \left(M_H M_L\right)^{m_2} M_H \\ M_{\mathrm{Fe}} \left(M_L M_H\right)^{m_1} M_{2L} \left(M_H M_L\right)^{m_2} M_H. \quad \text{(A1)}$$

Then the reflection and transmission coefficients are given by

$$r = \frac{Y_0 m_{11} + Y_0 Y_{sub} m_{12} - m_{21} - Y_{sub} m_{22}}{Y_0 m_{11} + Y_0 Y_{sub} m_{12} + m_{21} + Y_{sub} m_{22}}, \quad \text{(A2)}$$

$$t = \frac{2Y_0}{Y_0 m_{11} + Y_0 Y_{sub} m_{12} + m_{21} + Y_{sub} m_{22}}, \quad \text{(A3)}$$

where $Y_0 = \eta_0^{-1} = \sqrt{\varepsilon_0/\mu_0}$ and $Y_{sub} = n_{sub}\sqrt{\varepsilon_0/\mu_0}$ are the admittances for the incident region (air) and substrate, respectively.

In Eq. (A1), the characteristic matrix for Cr or Fe is given by

$$M_{\mathrm{Cr,Fe}} = \begin{pmatrix} \cos\left(k_0 h_{\mathrm{Cr,Fe}}\right) & \frac{j \sin\left(k_0 h_{\mathrm{Cr,Fe}}\right)}{Y_M} \\ jY_{\mathrm{Cr,Fe}} \sin\left(k_0 h_{\mathrm{Cr,Fe}}\right) & \cos\left(k_0 h_{\mathrm{Cr,Fe}}\right) \end{pmatrix}, \quad \text{(A4)}$$

where the admittance is

$$Y_{\mathrm{Cr,Fe}} = Y_0 n_{\mathrm{Cr,Fe}} \cos\theta_{\mathrm{Cr,Fe}} \text{ (TE-wave)}, \tag{A5}$$

$$Y_{\mathrm{Cr,Fe}} = \frac{Y_0 n_{\mathrm{Cr,Fe}}}{\cos\theta_{\mathrm{Cr,Fe}}} \text{ (TM-pwave)}, \tag{A6}$$

respectively, and the optical thickness is $h_{\mathrm{Cr,Fe}} = n_{\mathrm{Cr,Fe}} d \cos\theta_{\mathrm{Cr,Fe}}$ where $n_{\mathrm{Cr,Fe}}$ is the refractive index; d is the thickness of the metal film; $k_0 = 2\pi/\lambda$ is the free-space wavenumber.

As for the quarter-wave$H$ and L layers, their characteristic matrices are

$$M_L = \begin{bmatrix} \cos(k_0 n_L d_L \cos\theta_L) & \frac{j\sin(k_0 n_L d_L \cos\theta_L)}{Y_L} \\ jY_L \sin(k_0 n_L d_L \cos\theta_L) & \cos(k_0 n_L d_L \cos\theta_L) \end{bmatrix}, \tag{A7}$$

$$M_H = \begin{bmatrix} \cos(k_0 n_H d_H \cos\theta_H) & \frac{j\sin(k_0 n_H d_H \cos\theta_H)}{Y_H} \\ jY_H \sin(k_0 n_H d_H \cos\theta_H) & \cos(k_0 n_H d_H \cos\theta_H) \end{bmatrix}, \tag{A8}$$

where $n_L d_L = n_H d_H = \lambda_0/4$ with λ_0 being the design wavelength, and Y_L, Y_H are defined as in Eqs. (A5) and (A6) with Cr, Fe $\rightarrow L, H$, respectively.

ACKNOWLEDGMENT

C.-J. Wu acknowledges the financial support from the National Science Council of the Republic of China under Contract No. NSC-97-2112-M-003-013-MY3.

REFERENCES

1. Orfanidis, S. J., *Electromagnetic Waves and Antennas*, Chapter 7, Rutger University, 2008. www.ece.rutgers.edu/∼orfanidi/ewa.
2. Gamble, R. and P. H. Lissberger, "Reflection filter multilayers of metallic and dielectric thin films," *Appl. Opt.*, Vol. 28, 2838–2846, 1989.
3. Sheng, J.-S. and J.-T. Lue, "Ultraviolet narrow-band rejection filters composed of multiple metal and dielectric layers," *Appl. Opt.*, Vol. 31, 6117–6121, 1992.
4. Tan, M. Q., Y. C. Lin, and D. Z. Zhao, "Reflection filter with high reflectivity and narrow bandwidth," *Appl. Opt.*, Vol. 36, 827–830, 1997.
5. Augustsson, T., "Proposal of a DMUX with a Fabry-Perot all-reflection filter-based MMIMI configuration," *IEEE Photonics Technol. Lett.*, Vol. 13, 215–217, 2001.

6. Sun, X. Z., P. F. Gu, W. D. Shen, X. Liu, Y. Wang, and Y. G. Zhang, "Design and fabrication of a novel reflection filter," *Appl. Opt.*, Vol. 46, 2899–2902, 2007.
7. Shen, W., X. Sun, Y. Zhang, Z. Luo, X. Liu, and P. Gu, "Narrow band filter in both transmission and reflection with metal/dielectric thin films," *Optics Comm.*, Vol. 282, 242–246, 2009.
8. Chang, Y.-H., C.-C. Liu, T.-J. Yang, and C.-J. Wu, "Angular dependent of a narrow band reflection-and-transmission filter containing a ultra thin metallic film," *J. Opt. Soc. Am. B: Optical Physics*, Vol. 26, 1141–1145, 2009.
9. Wu, C.-J., B.-H. Chu, M.-D. Weng, and H.-L. Lee, "Enhancement of bandwidth in a chirped quarter-wave dielectric mirror," *Journal of Electromagnetic Waves and Applications*, Vol. 23, 437–447, 2009.
10. Srivastava, R., S. Pati, and S. P. Ojha, "Enhancement of omnidirectional reflection in photonic crystal heterostructure," *Progress In Electromagnetics Research B*, Vol. 1, 197–208, 2008.
11. Wang, X., X. Hu, Y. Li, W. Jia, C. Xu, X. Liu, and J. Zi, "Enlargement of omnidirectional total reflection frequency range in one-dimensional photonic crystals by using photonic heterostructures," *Appl. Phys. Lett.*, Vol. 80, 4291–4293, 2002.
12. Moghimi, M. J., H. Ghafoori-Fard, and A. Rostami, "Analysis and design of all-optical switching in apodized and chirped bragg gratings," *Progress In Electromagnetics Research B*, Vol. 8, 87–102, 2008.
13. Saliminejad, R. and M. R. Ghafouri Fard, "A novel and accurate method for designing dielectric resonator filter," *Progress In Electromagnetics Research B*, Vol. 8, 293–306, 2008.
14. Yeh, P., *Optical Waves in Layered Media*, John Wiley & Sons, Singapore, 1991.
15. João R. Canto, Sérgio A. Matos, Carlos R. Paiva, and Afonso M. Barbosa, "Effect of losses in a layered structure containing DPS and DNG media," *PIERS Online*, Vol. 4, No. 5, 546–550, 2008.
16. Born, M. and E. Wolf, *Principles of Optics*, Cambridge, London, 1999.
17. Hecht, E., *Optics*, Chapter 9, Addison Wesley, New York, 2002.